

## Determination of the electronic structure of transition-metal compounds: 2*p* x-ray photoemission spectroscopy of the nickel dihalides

J. Zaanen, C. Westra, and G. A. Sawatzky

*Laboratory of Physical Chemistry, Materials Science Center, University of Groningen,  
Nijenborgh 16, NL-9747 AG Groningen, The Netherlands*

(Received 14 August 1985; revised manuscript received 7 February 1986)

A recently proposed impuritylike many-body theory for the electronic structure of transition-metal compounds is extended to core photoemission. The theory is worked out in detail for the nickel dihalides, and we compare the results with experimental 2*p* spectra. We show that these spectra can be used for a quantitative determination of the parameters in the theory. We furthermore show that the easy-to-handle cluster model is a fair approximation to the full theory as far as core x-ray photoemission is concerned. We find that the Coulomb interaction energies are the largest energies in the system, and we show that the order of magnitude of these can be estimated from an ionic screening model. Furthermore we show that the charge-transfer energies strongly vary along the series. A comparison with estimates for the parameters derived from other experiments show systematic discrepancies. We argue that these are due to the neglect of higher-order interactions in the model Hamiltonian used.

### I. INTRODUCTION

Compounds of Ni such as the halides and chalcogenides have been the subject of numerous—both experimental and theoretical—investigations because of the obvious breakdown of the one-particle-potential band-structure description of their electronic structures and the related physical properties.

This is clearly demonstrated by a comparison of recent band-structure calculations<sup>1</sup> and valence-band photoemission and inverse-photoemission measurements on NiO.<sup>2,3</sup> The experimental results for NiO clearly show that the *d-d* Coulomb interactions dominate over bandwidths and hybridization interactions to such a large extent that an independent-electron description of the excited states breaks down completely.

The most obvious consequence of the importance of *d-d* correlation are the large charge-transport gaps in many transition-metal compounds (TMC's) as suggested by Mott as early as 1949.<sup>4</sup> Inspired by the photoemission work, we recently proposed a generalization of the Mott-Hubbard theory<sup>4,5</sup> in order to account for the systematics of the charge-transport gap in the compounds of 3*d* metals.<sup>6</sup> In this theory, a large *d-d* Coulomb interaction ( $U$ ) is a necessary but not sufficient condition to obtain a finite gap. For large  $U$  in the late-3*d*-transition-metal compounds the presence and magnitude of a band gap is basically determined by the charge-transfer energy ( $\Delta$ ), the energy cost to transfer an electron from the ligand to the metal ion. The further parameters in the model are the ligand *p*-band width ( $W$ ) and the *p-d* hybridization ( $T$ ). The basic assumption in this theory is that at least for the insulators the dynamics of the system can be divided into two energy scales. There is a large energy scale which involves charge degrees of freedom which determine, for instance, the charge-transport gap. The translational symmetry of the metal ions is, for this, of secondary impor-

tance and accurate results can be obtained by considering a single metal ion in a matrix of ligand ions (impurity approximation). Virtual charge excitations couple, however, the spins on different metal ions as explained by Anderson's superexchange theory,<sup>7</sup> which gives rise to a low-energy scale which can be treated by spin-only (Heisenberg) Hamiltonians.

One of the probes sensitive to the high-energy scale of the problem is core photoemission. The basic phenomenon we measure with this technique is the response of the valence-electron system to the sudden creation of a core-hole.

If the interaction between the core hole and the (correlated) valence electrons is sufficiently strong, satellites accompanying the main lines are observed in the photoemission spectra. In nearly all insulating transition-metal compounds prominent satellite structures are observed.<sup>8-29</sup> It is then interesting that large variations are seen in the satellite structure, depending on the compound under consideration (see, e.g., Fig. 1). This opens the possibility to use core x-ray photoemission (XPS) as a probe for the electronic structure in these materials.

The central problem in the analysis of these spectra is that one needs first a fair understanding of the nature of the many-body problem in these systems before an attempt can be made to understand the above-mentioned trends. van der Laan *et al.* in their paper on the copper dihalides<sup>24</sup> were the first to give a quantitative interpretation of core-photoemission spectra of TMC's in terms of a well-founded model. At this point we would stress that the earlier attempts<sup>25</sup> were in terms of independent-(valence-) electron theory, while van der Laan *et al.* were the first to follow a configuration-interaction approach.

For the specific case of Cu(II) compounds the differences between these two approaches are largely hidden because we are dealing with a one-particle problem in the ground state<sup>6</sup> and (under the neglect of the internal core-

hole degrees of freedom) a one-particle problem in the core-ionized state. If we are dealing with a transition-metal (TM) ion different from  $\text{Cu}^{2+}$ , the ground state of the system is a more-than-one-particle problem and then it is necessary to use a configuration-interaction (CI) approach in order to understand the spectra.

From the work of Gunnarsson and Schönhammer,<sup>30</sup> and others,<sup>31-34</sup> for the related Ce intermetallics and  $\text{CeO}_2$ , it is already clear that such a many-body approach gives meaningful quantitative results. In this paper we will show that also the core-photoemission spectra of the Ni compounds can be understood in detail within the Anderson impurity framework.

We already noticed that the differences between the core spectra of different TM compounds are quite large. These variations follow naturally from the theoretical model. From the parameters which control the large energy scale in the transition-metal compounds,<sup>6</sup> the Coulomb interactions as well as the ligand bandwidth and the hybridizations are expected to be roughly constant along the halide series, while the Ni-ligand charge-transfer energy will strongly vary. This then gives rise to a large diversity of ionized-state electronic structures which explain the experimental observation.

This large variation enables us to analyze these spectra in considerable detail and to determine the parameters of the theory. Comparing these values with the values needed for the band-gap magnitudes and other experiments, we find that, although the trends are consistent, systematic discrepancies occur. We argue that these can be attributed to a number of higher-order interactions, which are not included in the simplest version of the impurity model.

The organization of this paper is as follows. In Sec. II we present experimental results for the  $2p$  XPS spectra and discuss some properties of the materials. In Sec. III we go into the cluster approximation, which is the zero-ligand-bandwidth approximation of the impurity problem. This is quite a fair approximation for core XPS and because it is very easy to handle it can be used to derive order-of-magnitude estimates for the parameters determining the electronic structure. In Sec. IV we derive the full impurity-approximation results and finally, in Sec. V, we compare these with the experimental results and give a thorough discussion of the parameters as derived in this way.

## II. MATERIALS AND EXPERIMENTAL DETAILS

The Ni ions in the Ni dihalides are located in a distorted octahedron formed by the nearest-neighbor anions. The distortion is rhombohedral in  $\text{NiCl}_2$ ,  $\text{NiBr}_2$ , and  $\text{NiI}_2$  with space group  $D_{3d}^5$  ( $R\bar{3}m$ ). These materials can be considered as layered compounds with the Ni layers alternating with a double layer of halogen atoms. The crystal structure of  $\text{NiF}_2$  is somewhat different. Here the distortion is tetragonal in a  $D_{4h}$  space group. Important for us is that the local surrounding of the Ni ion is close to octahedral and we will subsequently neglect the small distortions.

All of the materials are large-band-gap insulators with

$\text{NiI}_2$  having the smallest optical gap of about 1.7 eV.<sup>35</sup> Above 200 K the materials are paramagnetic with magnetic moments on the Ni ions close to the expected high spin value of  $2\mu_B$ . Magnetic ordering sets in at low temperature where the materials order antiferromagnetically but, in some cases, with complicated spin structures.

The materials used in this study were either obtained commercially ( $\text{NiF}_2$  and  $\text{NiCl}_2$ ) or prepared in the laboratory of inorganic chemistry ( $\text{NiBr}_2$  and  $\text{NiI}_2$ ). Before use the materials were heated to 500°C in vacuum for a period of 2 d to remove the water. Measurements were done on both sublimed thin films prepared *in situ* and powders prepared in a glove box attached to the spectrometer. No difference, except for changes in charging, were observed using these two methods. The charging was determined by both the thin-film measurements and by referencing to the O  $1s$  line at 531.7 eV binding energy (BE). The always-present weak O  $1s$  line was certainly a result of some water remaining in the samples.

The XPS spectra were collected with an AEI (Kratos) ES200 spectrometer modified for ultrahigh vacuum. During the measurements the vacuum was in the low- $10^{-10}$ -Torr range. The spectra shown are obtained using Mg  $K\alpha$  radiation. The core-line spectra were corrected for a scattered electron background, x-ray satellites, and the analyzer transmission function using a procedure described elsewhere.<sup>36</sup>

In Fig. 1 we show the XPS spectra of the Ni  $2p$  region of the Ni dihalides. The  $\text{NiCl}_2$ ,  $\text{NiBr}_2$ , and  $\text{NiI}_2$  exhibit two satellite lines in the Ni  $2p_{3/2}$  and Ni  $2p_{1/2}$  energy regions. The  $2p_{1/2}$  NiI<sub>2</sub> region is largely obscured by the I  $3p$  line.  $\text{NiF}_2$  exhibits only one satellite and the whole spectrum is severely broadened [full width at half maximum (FWHM) of  $\approx 4.0$  eV], probably due to charging.

We notice that the satellite structure in the  $2p_{3/2}$  and  $2p_{1/2}$  regions is considerably different. In the following paper<sup>37</sup> we have shown that this is due to strong interference effects in the Ni  $2p^{1/2}$  spectrum because of low-energy Coster-Kronig continua. We will therefore restrict

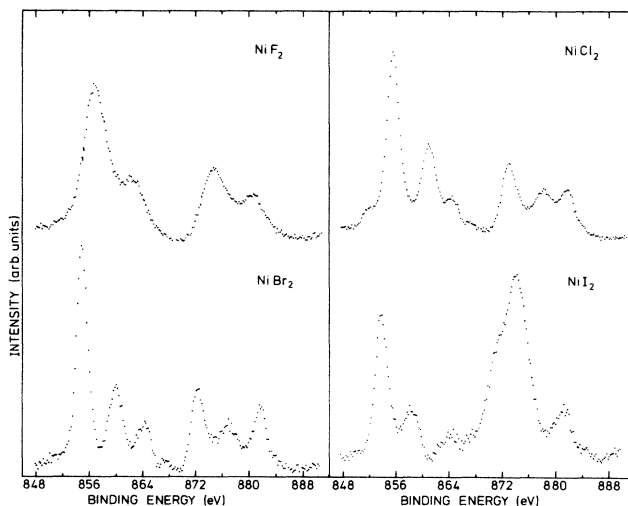


FIG. 1.  $2p$  XPS spectra of the Ni dihalides. The spectra are corrected for background, analyzer transmission, and charging. The  $2p_{1/2}$  spectrum of  $\text{NiI}_2$  is obscured by the I  $3p$  line.

TABLE I. Measured peak positions and intensities of the  $2p$  spectra of the Ni dihalides. Intensity ratios are determined from peak areas. ? denotes unknown values.

	$E_1$	$E_2$	$\frac{2p_{3/2}}{I_2/I_1}$	$E_3$	$I_3/I_1$	$E_1$	$E_2$	$\frac{2p_{1/2}}{I_2/I_1}$	$E_3$	$I_3/I_1$
NiF <sub>2</sub>	857	862.5	0.33			875.	880.5	0.64		
NiCl <sub>2</sub>	855.6	861.1	0.51	864.6	0.17	873.1	878.2	0.94	881.9	0.54
NiBr <sub>2</sub>	854.7	859.7	0.48	864.0	0.28	872.0	876.6	0.79	881.3	0.88
NiI <sub>2</sub>	853.4	857.8	0.29	863.9	0.18	?	?	?	?	?

our discussion here to the  $2p_{3/2}$  energy region, which is not affected by interference effects.

In Table I we list the binding energies of the  $2p$  lines and the satellite intensities relative to the main line determined from the areas. These numbers were derived by fitting the spectra to a sum of three Lorentzians.

### III. THE CLUSTER APPROXIMATION

Before we go into the full impurity theory we will first present the results of a cluster calculation. The cluster approximation is a good first order approximation to the full theory and is more transparent with respect to the physics involved. In the cluster approximation we idealize the structure with the Ni at the center of an octahedron of anions.

For a purely ionic Ni(II)-compound the ground state would be a  $d^8(^3F)$  configuration and because of the large crystal field splitting the ground state would be  $^3A_{2g}$  with two holes in  $e_g$  orbitals. The purely ionic configuration then is  $|d_{x^2-y^2}d_{3z^2-r^2}|$  for the  $M_S=1$  state ( $d_{x^2-y^2}$  denotes a hole in this  $e_g$  orbital). This state can mix with ligand hole states of the same symmetry which we can consider to be composed of a linear combination of  $p_z$  orbitals on the anions.<sup>38</sup> We define ligand-hole wave functions

$$\begin{aligned} \underline{L}_{x^2-y^2} &= \frac{1}{\sqrt{4}}(p_{z_1} + p_{z_3} - p_{z_2} - p_{z_4}), \\ \underline{L}_{3z^2-r^2} &= \frac{1}{\sqrt{8}}(2p_{z_5} + 2p_{z_6} - p_{z_1} - p_{z_2} - p_{z_3} - p_{z_4}). \end{aligned} \quad (1)$$

We will then, for the ground state, have to deal with a three-level problem,<sup>2</sup>

$$\begin{aligned} |d^8\rangle &= |d_{x^2-y^2}d_{3z^2-r^2}|, \\ |d^9\underline{L}\rangle &= \frac{1}{\sqrt{2}}(|d_{x^2-y^2}\underline{L}_{3z^2-r^2}| + |\underline{L}_{x^2-y^2}d_{3z^2-r^2}|), \\ |d^{10}\underline{L}^2\rangle &= |\underline{L}_{x^2-y^2}\underline{L}_{3z^2-r^2}|. \end{aligned} \quad (2)$$

These are the only states which have  $^3A_{2g}(e_g^2)$  symmetry. The diagonal energies of these states are given by

$$\begin{aligned} \langle d^8 | H | d^8 \rangle &= 0, \\ \langle d^9\underline{L} | H | d^9\underline{L} \rangle &= \Delta, \\ \langle d^{10}\underline{L}^2 | H | d^{10}\underline{L}^2 \rangle &= 2\Delta + U, \end{aligned} \quad (3)$$

where  $\Delta$  is the charge-transfer energy which includes Madelung and polarization corrections as well as the  $d$ -electron ligand-hole Coulomb attraction. It should be

noted that the polarization contribution can be quite substantial for the localized  $d$  electron. In Eq. (3)  $U$  is the effective  $d$ - $d$  Coulomb interaction, which we can write as

$$U = U_0 - 2u - 2E_p, \quad (4)$$

where  $U_0$  is the bare  $d$ - $d$  Coulomb interaction,  $u$  is the  $d$ - $\underline{L}$  Coulomb attraction, and  $E_p$  is the polarization energy. The factor of 2 appears because the total polarization energy. The factor of 2 appears because the total polarization energy goes as  $Z^2$ , but  $2\Delta$  in Eq. (3) also includes  $2E_p$ , leaving  $2E_p$  for  $U$ . In addition, there will be off-diagonal matrix elements,

$$\langle d^8 | H | d^9\underline{L} \rangle = \sqrt{2}T, \quad \langle d^9\underline{L} | H | d^{10}\underline{L}^2 \rangle = \sqrt{2}T, \quad (5)$$

where

$$T = \langle d_{x^2-y^2} | H | \underline{L}_{x^2-y^2} \rangle = \langle d_{3z^2-r^2} | H | \underline{L}_{3z^2-r^2} \rangle, \quad (6)$$

and the  $\sqrt{2}$  enters because of degeneracy just as in a  $1/N_f$  expansion.<sup>33</sup>

In order to determine the ground-state wave function we must then diagonalize the matrix as defined by Eqs. (3) and (5).

The wave function of the ground state of the cluster can be written as

$$\Psi_G = A(|d^8\rangle + \alpha|d^9\underline{L}\rangle + \beta|d^{10}\underline{L}^2\rangle), \quad (7)$$

with  $A^2 = (1 + \alpha^2 + \beta^2)^{-1}$ .

These states and their hybridization are pictorially represented in Fig. 2, including the stabilization of the ground state due to hybridization ( $\delta$ ).

The  $|d^{10}\underline{L}^2\rangle$  occupation of the ground state will always be small because of the large  $U$  in the Ni compounds. Fluctuation between states  $|d^8\rangle$  and  $|d^9\underline{L}\rangle$  then remains. For strongly ionic compounds (NiF<sub>2</sub>)  $\Delta$  is large and the ground state will be very close to  $|d^8\rangle$ , while for more covalent compounds (NiI<sub>2</sub>)  $\Delta$  will be of the order of  $T$  and the ground state will be characterized by nearly equal weights of the  $|d^8\rangle$  and  $|d^9\underline{L}\rangle$  configurations.

We now turn to the problem of determining the eigenstates in the presence of the core hole. The final states are now of the form  $|\underline{c}d^8\rangle$ ,  $|\underline{c}d^9\underline{L}\rangle$ , and  $|\underline{c}d^{10}\underline{L}^2\rangle$ , where  $\underline{c}$  denotes a core hole. We define the diagonal energies as

$$\begin{aligned} \langle \underline{c}d^8 | H | \underline{c}d^8 \rangle &= E_c, \\ \langle \underline{c}d^9\underline{L} | H | \underline{c}d^9\underline{L} \rangle &= E_c + \Delta - Q, \\ \langle \underline{c}d^{10}\underline{L}^2 | H | \underline{c}d^{10}\underline{L}^2 \rangle &= E_c + 2(\Delta - Q) + U. \end{aligned} \quad (8)$$

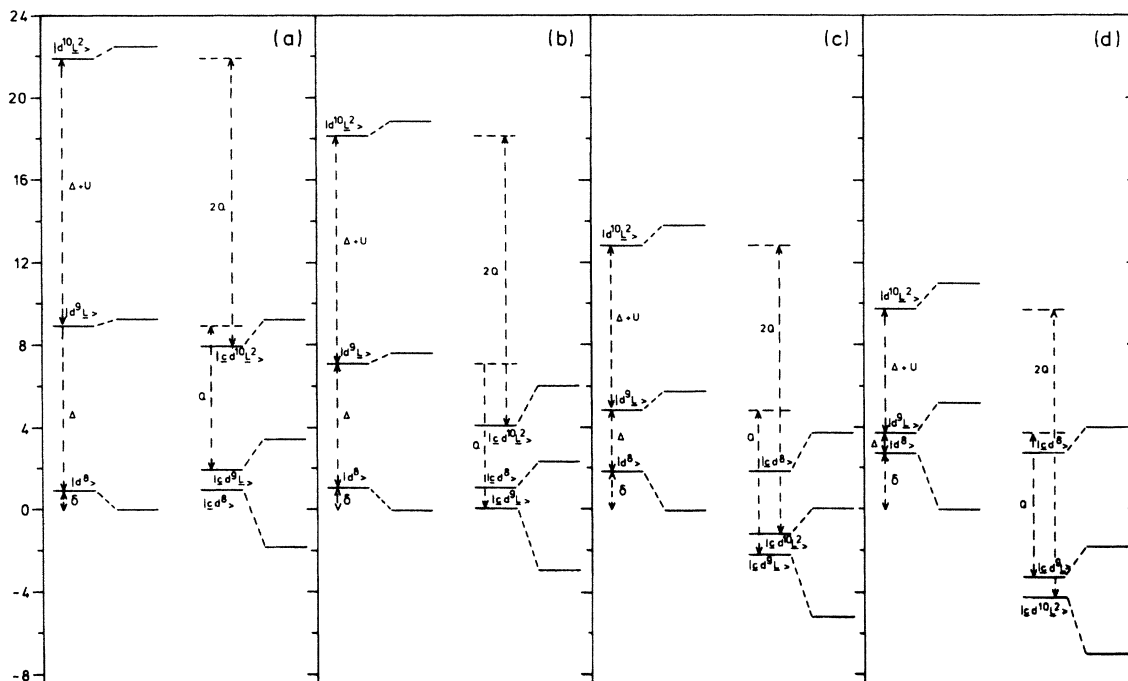


FIG. 2. The four possible level sequences in the core-ionized state and the corresponding neutral states as a function of  $\Delta$  in the cluster model. For the other parameters we took  $Q=7$  eV,  $U=5$  eV, and  $T=2$  eV. (a)  $\Delta=8$  eV, no level inversion takes place because  $\Delta > Q$ . (b)  $\Delta=6$  eV, level sequence in core-ionized state is  $E_{d^9} < E_{d^8} < E_{d^{10}}$  because  $Q > \Delta$  and  $2Q < 2\Delta + U$ . (c)  $\Delta=3$  eV, also  $E_{d^{10}} < E_{d^8}$  because  $2Q < 2\Delta + U$ , but still  $E_{d^{10}} > E_{d^9}$  because  $Q < \Delta + U$ . (d)  $\Delta=1$  eV, the level sequence is opposite from that in the ground state.

Here,  $E_c$  is defined relative to the ionic lattice and includes a Madelung ( $E_M$ ) and a polarization correction,

$$E_c = E_c^0 - E_p - E_M. \quad (9)$$

$Q$  is the core-hole- $d$ -electron Coulomb attraction, which, just as for  $U$  in the initial state, includes a polarization- and a core-hole  $L$ -hole repulsion ( $q$ ) correction,

$$Q = Q_0 - 2E_p - q. \quad (10)$$

As defined above,  $Q$  is positive and it lowers the energy of the  $d^9\bar{L}$  state as well as the  $d^{10}\bar{L}^2$  state relative to the  $d^8$  state.

The off-diagonal matrix elements are assumed to be the same as for the initial state, so again we must solve a  $3 \times 3$  problem as defined by (5) and (8).

The wave functions of the final states are given by

$$|\Psi_i\rangle = A_i(|\underline{cd}^8\rangle + \alpha'_i|\underline{cd}^9\bar{L}\rangle + \beta'_i|\underline{cd}^{10}\bar{L}^2\rangle). \quad (11)$$

In the sudden approximation the XPS spectrum will be given by

$$\rho(\xi_k) = \sum_{i=1}^3 |\langle \Psi_i | \underline{\Psi}_g \rangle|^2 \delta(\hbar\omega + \delta - \xi_k - E_i), \quad (12)$$

where  $E_i$  are the final-state energies,  $\hbar\omega$  the energy of the x rays, and  $\xi_k$  the kinetic energy of the photoelectron.  $|\underline{\Psi}_g\rangle$  represents the frozen state obtained by annihilating a core electron in the ground state.

Equation (12) can be rewritten, using (7) and (11), as

$$\rho(\xi_k) = \sum_{i=1}^3 (AA'_i)^2 (1 + \alpha\alpha'_i + \beta\beta'_i)^2 \delta(\hbar\omega + \delta - \xi_k - E_i). \quad (13)$$

With this result and having knowledge about the four parameters  $\Delta$ ,  $T$ ,  $U$ , and  $Q$ , we can calculate the cluster-approximation prediction for the XPS spectrum.

As we already noticed, the interaction with the core hole ( $Q$ ) tends to lower the energy of valence-electron configurations which were at high energy in the ground state ( $|d^9\bar{L}\rangle$ ,  $|d^{10}\bar{L}^2\rangle$ ). If  $Q$  is large enough the sequence of states in the core-ionized state can be quite different from that in the ground state, which can give rise to satellite structure.

Due to the particular electronic structure of the transition-metal compounds, the modification of the valence-electronic structure by the presence of the core hole gives rise to a large diversity in the final states as a function of the ligand electronegativity ( $\Delta$ ).

In order to show this, we work out a numerical example. We assume that  $U$  and  $Q$  as well as  $T$  are constant in the series. As we will see,  $U=5.0$  eV,  $Q=7.0$  eV, and  $T=2.0$  eV are good estimates for these quantities. Inserting these values in Eq. (8), we find

$$\langle \underline{cd}^8 | H | \underline{cd}^8 \rangle = 0,$$

$$\langle \underline{cd}^9\bar{L} | H | \underline{cd}^9\bar{L} \rangle = \Delta - 7,$$

and

$$\langle cd^{10}\underline{L}^2 | H | cd^{10}\underline{L}^2 \rangle = 2\Delta - 9.$$

As a function of  $\Delta$  one can now distinguish a number of different regimes. First, we have the regime  $\Delta > Q$ . As can be seen from Fig. 2 ( $\Delta = 8$ ), the level sequence in the core-ionized state is the same as in the initial state. Although the ground-state wave function of the core-ionized system is not exactly identical to the ground-state wave function of the neutral system, they both are of predominant  $d^8$  character. In this case we thus expect only a weak satellite, which shows that not only  $Q > T$  but also  $Q > \Delta$  are required to obtain prominent satellite features.

Second, we have the regime  $\Delta < Q$  and  $2\Delta + U > 2Q$ , which corresponds to the strongly ionic Ni compounds. As can be seen from Fig. 2(b) ( $\Delta = 6$ ), we find  $E_{d^{10}} > E_{d^8}, E_{d^9}$ . Because the  $|d^{10}\underline{L}^2\rangle$  configuration is not occupied in the ground state, the  $|cd^{10}\underline{L}^2\rangle$  final-state configuration cannot be reached. Furthermore, because  $\Delta < Q$  the level sequence of the  $d^8$  and  $d^9$  configurations is inverted in the final state with respect to the ground state. One thus expects an XPS spectrum consisting of a main line of predominant  $d^9\underline{L}$  character and a satellite of predominant  $d^8$  character separated by approximately  $\Delta - Q$ . This is the situation encountered in  $\text{NiF}_2$ , and also in  $\text{NiO}$ , where indeed a single satellite is observed. One should note that this is equivalent to the situation in the XPS spectra of the  $\text{Cu(II)}$  halides in the analysis of van der Laan *et al.*<sup>24</sup>

Considering now the strongly covalent materials ( $\Delta < Q - U$ , for instance, in  $\text{NiI}_2$ ), the final state looks completely different [Fig. 2(d),  $\Delta = 1$ ]. The  $|cd^{10}\underline{L}^2\rangle$  state is lowest in energy and corresponds thus to the fully relaxed peak in the XPS spectrum, while  $|cd^9\underline{L}\rangle$  is still lower in energy than  $|cd^8\rangle$ . All three eigenstates of the core-ionized state will now be visible in the XPS spectrum, which is in agreement with experiment. Reading for  $d^8 \rightarrow f^0$ ,  $d^9 \rightarrow f^1$ , and  $d^{10} \rightarrow f^2$ , one recognizes that the situation is equivalent to the one encountered in cerium compounds and intermetallic compounds.<sup>30-34</sup> On the  $\Delta$  scale we have, finally, the intermediate covalent materials ( $Q - U < \Delta < Q - \frac{1}{2}U$ ) as  $\text{NiBr}_2$  and  $\text{NiCl}_2$  [Fig. 2(c),  $\Delta = 4$ ]. Now the lowest eigenstate is of  $|cd^9\underline{L}\rangle$  character and the highest eigenstate of  $|cd^8\rangle$  character, while the  $|cd^{10}\underline{L}^2\rangle$  state is in between. We again expect three lines in the XPS spectrum, while the central line will show a strong shift as a function of  $\Delta$ . This is indeed observed if one compares the  $2p_{3/2}$  spectra of  $\text{NiCl}_2$  and  $\text{NiBr}_2$ .

As we will see in the next section, the cluster model is quite a good approximation to the full problem and it can certainly be used to obtain a good estimate of the magnitude of the parameters. In contrast to the impurity theory, which will be treated in the next section, the line positions and intensities are well defined within the cluster model. This facilitates a parameter search because we can plot curves of line positions and line intensities as a function of  $\Delta$ ,  $U$ ,  $Q$ , and  $T$ .

These are shown in Figs. 3(a) and 3(b). In Fig. 3(a) we plot the separation of the first and second satellite with the main (lowest-BE) line. In Fig. 3(b) we plot the intensity of both satellites with respect to the main-line intensity. In both panels (a) and (b) all energies are in units of  $T$  and

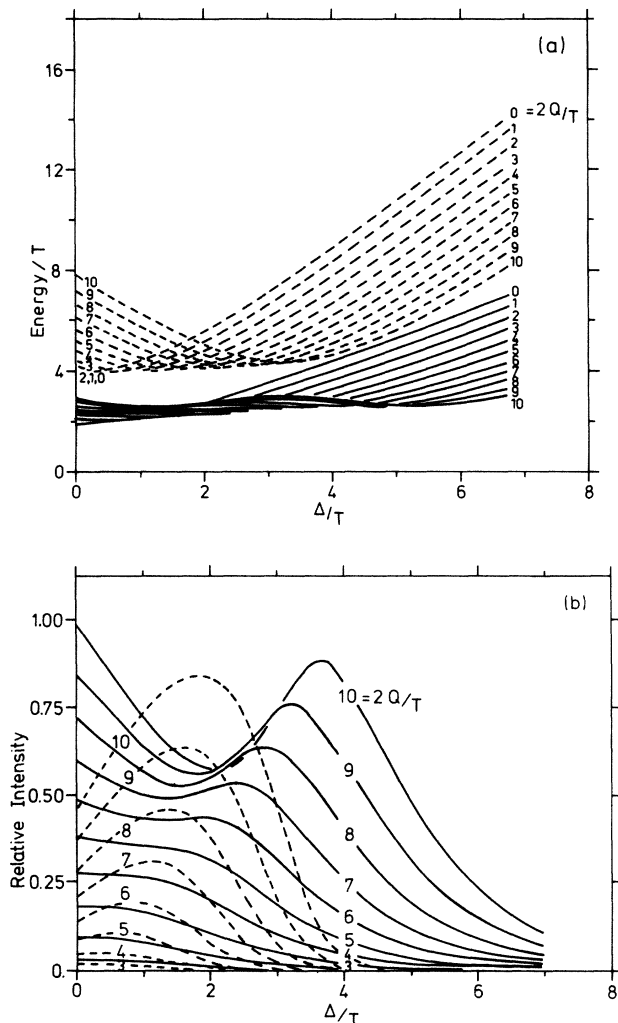


FIG. 3. XPS spectra calculated from the cluster model as a function of  $\Delta/T$  for different values of  $2Q/T$  and  $U = 0.7Q$ . (a) Solid line gives the position of the lower-energy satellite relative to the main line in units of  $T$ , the dashed line the same for the higher-energy satellite. (b) Solid line gives the ratio of the intensity of the lower-energy satellite and the main-line intensity, the dashed broken line the same for the higher-energy satellite.

we took  $U/Q = 0.7$ , which will be, in most cases, appropriate, as we will show in the next section. We took the parameter range such that it is representative for the parameter values of Ni compounds. With some caution these curves can also be used to estimate the parameters appropriate for compounds of other (Co, Fe, Mn) transition-metal compounds.

We can use these figures to obtain good estimates of the various parameters for the Ni dihalides. The relative intensity of the first satellite in  $\text{NiCl}_2$  from Table I is 51%, which according to Fig. 2 puts  $Q/T \approx 3.5$  and  $1 < \Delta/T < 2$ . This—combined with the 17% intensity of the second satellite—gives  $\Delta/T \approx 2$ . Looking then at Fig. 1 and the satellite energies of Table I, we obtain  $T \approx 2$ . The increase in the second-satellite intensity in  $\text{NiBr}_2$  is obtained by staying on the  $Q/T = 3.5$  curve and decreasing  $\Delta/T$  to about 1.4 which, as observed, hardly causes a

change in the first-satellite intensity and decreases the first-satellite energy and increases the second-satellite energy to the observed values again for  $T=2$ . The observation of only one satellite in  $\text{NiF}_2$  is consistent with larger values of  $\Delta/T$  and the energy and intensity is consistent with  $T=2$ ,  $Q/T=3.5$ , and  $\Delta/T \approx 3.5$ .

#### IV. THE IMPURITY APPROXIMATION

Having gained some physical insight into the problem, we now continue with the impurity approximation. As band-structure calculations show,<sup>1,39</sup> the single-particle electronic structure is composed of a  $d$  band at the Fermi surface split up by the crystal-field interaction in an occupied  $t_{2g}$  band and a half-filled  $e_g$  band, both with a dispersive width on the order of 0.5 eV. Beneath the Fermi surface one has an occupied band of ligand  $p$  character. The width of this band is 3.0–4.0 eV, almost entirely due to ligand-ligand hybridization, and the center of this band shifts to the Fermi surface for a decreasing ligand electronegativity. Finally, well above the Fermi surface (5.0–6.0 eV) one has empty metal and ligand  $s-p$  densities of states.

The first approximation is to neglect the empty  $s-p$  states. This is a good approximation because of the small coupling between these and the Ni  $d$  states and because of the large excitation energies involved. Neglecting, furthermore, the  $d-d$  overlap, the system is well described by the Anderson lattice Hamiltonian,

$$\begin{aligned} H_0 &= \sum_{k,\sigma} \epsilon_{k\sigma} c_{k\sigma}^\dagger c_{k\sigma}, \\ H_d &= \sum_{i,m,\sigma} \epsilon_{dm} d_{im\sigma}^\dagger d_{im\sigma} + \sum_{i,k,l,x,y} U(k,l,x,y) d_{ik}^\dagger d_{il} d_{ix}^\dagger d_{iy}, \\ H_{\text{mix}} &= \sum_{i,k,m,\sigma} (V_{ikm} d_{im\sigma}^\dagger c_{k\sigma} + \text{h.c.}), \\ H &= H_0 + H_d + H_{\text{mix}}. \end{aligned} \quad (14)$$

$H_0$  describes the "host" band structure, which in our case involves the anion  $p$  band.  $H_d$  describes the  $d$ -electronic structure of a Ni ion at lattice site  $i$  in the point-group symmetry of the solid, including crystal-field splitting, and  $U$  describes the  $d-d$  Coulomb and exchange interactions which can be expressed in terms of the Slater integrals  $F_0$ ,  $F_2$ , and  $F_4$ .  $H_{\text{mix}}$  describes the hybridization between the  $d$  states of the impurity at site  $i$  and the host states.

This Hamiltonian takes fully into account the translational symmetry. Apart from the ligand  $np$  electrons which are written as Bloch functions in (17), also the translational symmetry of the  $d$  electrons is taken into account by the lattice summation ( $i$ ). This Hamiltonian constitutes a yet unsolved problem. The central approximation we make is that we neglect the translational symmetry of the transition-metal ions,<sup>6</sup> ending up with the problem of a single  $d$  impurity embedded in a filled-band host, which can be solved exactly. In the zero-ligand-bandwidth limit this Hamiltonian describes the cluster as introduced in Sec. III.

In order to simplify the situation we introduce some further model assumptions. To get rid of the  $k$  depen-

dence of the hybridization, we assume, following Bringer and Lustfeld<sup>40</sup> and Gunnarsson and Schönhammer,<sup>30</sup>

$$H_{\text{mix}} = \sum_{m,\sigma} [V(\epsilon) d_{m\sigma}^\dagger c_{\epsilon m\sigma} + \text{h.c.}] d\epsilon. \quad (15)$$

With the underlying assumption

$$\begin{aligned} \sum_k V_{km}^* V_{km} \delta(\epsilon - \epsilon_k) &= \sum_k |V_k|^2 \delta(\epsilon - \epsilon_k) \delta_{mm'}, \\ &= |V(\epsilon)|^2 \delta_{mm'}, \end{aligned} \quad (15a)$$

and

$$c_{\epsilon m\sigma}^\dagger = V(\epsilon)^{-1} \sum_k V_{km\sigma}^* \delta(\epsilon - \epsilon_k) c_{k\sigma}^\dagger. \quad (15b)$$

In principle, the details of the Coulomb and exchange interactions between the  $d$  electrons can be taken fully into account. For the  ${}^3A_{2g}$  ground state things are trivial and we will show in future publications that it is relatively straightforward to include multiplet interactions in similar calculations as presented here for the optical- and the x-ray-absorption spectra<sup>41</sup> of Ni compounds. In the calculation of the core XPS spectra we have to deal, however, with configurations containing one core hole and two  $d$  holes. This constitutes a difficult multiplet problem<sup>42–46</sup> and it is then a formidable task to give a full account of the configuration interaction in the core-ionized state. We therefore neglect the higher-order Coulomb and exchange interactions and write, for the core-hole- $d$ -electron interaction,

$$H_c = \sum_m Q(1 - n_c) d_m^\dagger d_m,$$

$n_c$  being the core-electron number operator and  $Q = F_0$  ( $2p\ 3d$ ).

Because of the filled ligand band and the half-filled  $e_g$  band, we have in the impurity approximation two hole degrees of freedom; in other words, we have a two-particle problem which can be solved exactly. We adopt a shorthand notation  $1 \rightarrow d_{3z^2-r^2}$  and  $2 \rightarrow d_{x^2-y^2}$  for the angular-momentum quantum numbers and, as a zero order, we take

$$|d^8\rangle = d_{11} d_{21} |\phi\rangle, \quad (16)$$

where  $|\phi\rangle$  is the filled ligand band and the filled  $d$  shell. Equation (16) represents the  $M_S=1$  ( ${}^3A_{2g}$ ) ionic state as in the cluster approximation.

We also have states with a hole transferred to the ligand band,

$$|d^9\epsilon\rangle = \frac{1}{\sqrt{2}} (d_{11}^\dagger c_{\epsilon 11} + d_{21}^\dagger c_{\epsilon 21}) |d^8\rangle, \quad (17)$$

and states with both holes transferred to the ligand band,

$$|d^{10}\epsilon\epsilon'\rangle = \frac{1}{\sqrt{2}} d_{11}^\dagger d_{21}^\dagger (c_{\epsilon 11} c_{\epsilon' 21} + c_{\epsilon 21} c_{\epsilon' 11}) |d^8\rangle, \quad (18)$$

with, as can be seen,  $\epsilon \leq \epsilon'$  in order to prevent overcompleteness.

The states (16)–(18) establish a complete basis set for the ground state of the impurity problem. Projecting Hamiltonian (15) onto this Hilbert space, we find the nonzero matrix elements

$$\begin{aligned}
\langle d^8 | H_{\text{imp}} | d^8 \rangle &= 0, \\
\langle d^9 \epsilon | H_{\text{imp}} | d^9 \epsilon' \rangle &= \delta(\epsilon - \epsilon') (\Delta + \epsilon), \\
\langle d^{10} \epsilon \epsilon' | H_{\text{imp}} | d^{10} \epsilon'' \epsilon''' \rangle &= \delta(\epsilon - \epsilon'') \delta(\epsilon' - \epsilon''') \\
&\quad \times (2\Delta + U + \epsilon + \epsilon'),
\end{aligned} \tag{19}$$

$$\langle d^8 | H_{\text{imp}} | d^9 \epsilon \rangle = \sqrt{2} V(\epsilon), \tag{20a}$$

$$\langle d^9 \epsilon | H_{\text{imp}} | d^{10} \epsilon' \epsilon'' \rangle = \sqrt{2} V(\epsilon) \delta(\epsilon - \epsilon') \delta(\epsilon - \epsilon'') + [1 - \delta(\epsilon' - \epsilon'')] [V(\epsilon'') \delta(\epsilon - \epsilon') + V(\epsilon') \delta(\epsilon - \epsilon'')]. \tag{20b}$$

Due to complications arising from the coupling to  $|d^{10} \epsilon \epsilon'\rangle$  states [Eq. (20b)], it is not possible to obtain easy to evaluate analytical solutions for the ground-state wave function. This is discussed extensively by Gunnarsson and Schönhammer in their treatment of the closely related problem of the strongly correlated impurity including double occupation in  $1/N$  theory.<sup>30,47</sup>

However, because the  $|d^{10} \epsilon \epsilon'\rangle$  are in most cases well split off from the other states, one feels that approximations should be possible. In the Appendix we work out such an approximation which yields good results for the ground state, at least as long as  $\Delta + U \gtrsim W$ . In the paper about XAS (Ref. 41) we used these approximate results, but in this paper we prefer an exact numerical approach.

In the numerical approach one divides the ligand band into  $N_\epsilon$  discrete states. The complete Hilbert space spanned by the impurity Hamiltonian then has a dimension of

$$N = 1 + 2N_\epsilon + N_\epsilon(N_\epsilon - 1)/2.$$

For fully converged solutions ( $20 \lesssim N_\epsilon \lesssim 100$ ), one has to diagonalize huge matrices for which conventional diagonalization methods are inappropriate.

However, very recently Gunnarsson and Schönhammer<sup>47</sup> proposed a method for the calculation of the ground-state wave function which is very efficient under the condition that the matrix is sufficiently sparse, as in our case. This method, based on the properties of Chebyshev polynomials, involves repeated matrix multiplications which can be carried out relatively fast because of the sparseness of the Hamiltonian matrix. It turns out that the effort is essentially proportional to  $N$ , in contrast to a diagonalization for which the work is proportional to  $N^3$ . The second advantage of this method is that storage of only  $3N$  numbers is required, while diagonalization requires storage of a  $N \times N$  matrix, which would be quite unfeasible. Having obtained in this way the ground-state wave function, it is then straightforward to calculate the ground-state energy  $\delta_n$  and the occupation numbers.

Aside from the ground-state covalent stabilization energy, also the  $d$  occupancy in the ground state is an interesting property. Defining  $|\Phi\rangle$  as the ground-state wave function composed from states (16)–(18), we have

$$\langle n_{d^8} \rangle = |\langle \Phi_0 | d^8 \rangle|^2, \tag{21a}$$

$$\langle n_{d^9} \rangle = \int_{-W/2}^{W/2} |\langle \Phi_0 | d^9 \epsilon \rangle|^2 d\epsilon, \tag{21b}$$

with  $-\frac{1}{2}W \leq \epsilon \leq \frac{1}{2}W$ .

$\Delta$  is defined as  $\epsilon_d - \epsilon_L$ , with  $\epsilon_L$  referring to the center of the ligand band with a width  $W$ . Note that we include in  $\Delta$  the stabilization of the  ${}^3A_{2g} |d^8\rangle$  state due to the  $F_2$  and  $F_4$  Slater integrals. Furthermore, we have the nondiagonal matrix elements

which are the probabilities of finding two- and one hole, respectively, on the Ni ion in the ground state. Using a semielliptical form for  $|V(\epsilon)|^2$ ,

$$\pi |V(\epsilon)|^2 = \frac{2T^2}{\frac{1}{4}W^2} (\frac{1}{4}W^2 - \epsilon^2)^{1/2}, \tag{22}$$

which should be compared with the actual  $e_g$ -projected ligand  $np$  density of states, we calculate the ground-state wave function and energy.

In Fig. 4 we show the result for the hybridization energy  $\delta$  and compare this quantity with the result of the cluster calculation as obtained from Eqs. (3) and (5). In Fig. 5 we show the results for  $\langle n_{d^8} \rangle$  and  $\langle n_{d^9} \rangle$ , which are compared with cluster results for these quantities. From these figures it can be concluded that for large  $\Delta$ 's (and  $U$ 's), as compared to the bandwidth, the cluster approach is a good approximation to the full impurity approximation. This is no longer true for small  $\Delta$ 's where strong deviations are noticed. For instance, we see a fast drop of the  $d^8$  content of the ground state for values of  $\Delta$  smaller than about  $\frac{1}{2}W$ , which is due to the tendency to drop a hole in the ligand band, giving rise to so-called  $p$ -type metals, as we have argued before.<sup>6</sup>

We now proceed with the calculation of the core XPS spectrum in the impurity approximation. In the sudden

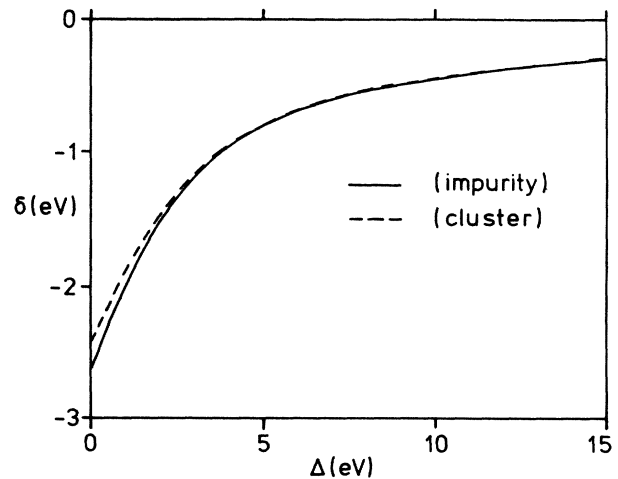


FIG. 4. Hybridization energy ( $\delta$ ) of the ground state as a function of  $\Delta$  for  $T=1.5$  eV,  $U=5$  eV, and  $W=3$  eV. Solid line indicates impurity result and dashed line indicates the cluster result.

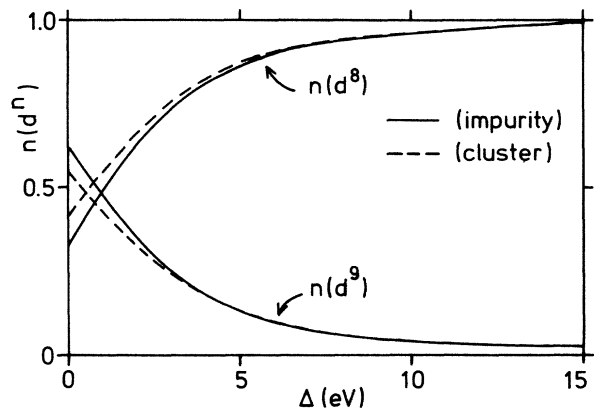


FIG. 5.  $d^8$  and  $d^9$  counts for the same parameter values as used for Fig. 4. Solid line is impurity result and dashed line is derived from the cluster model.

approximation the core-level photoemission current is directly related to the core spectrum,

$$j(\xi) = \frac{1}{\pi} \text{Im} G_c(z - \hbar\omega), \quad (23)$$

$$G_c(z) = \left\langle \Psi_0 \left| p_c^\dagger \frac{1}{z + \delta - H} p_c \right| \Psi_0 \right\rangle, \quad (24)$$

and  $z = \xi - iy$ . In (24),  $p_c^\dagger$  creates a core electron and  $\delta$  is the ground-state energy.

In Eq. (24)  $H$  includes the core-hole- $d$ -electron Coulomb interaction. We will evaluate (24) in the Hilbert space spanned by the states  $|\underline{c}d^8\rangle = p_c |d^8\rangle$ ,  $|\underline{c}d^9\epsilon\rangle$ , and  $|\underline{c}d^{10}\epsilon\epsilon'\rangle$ , and the matrix elements in this basis are given by (19) and (20), except that  $\Delta \rightarrow \Delta - Q$ , as in the cluster model. The Green's function can be found, in principle, by matrix inversion. However, Gunnarsson and Schönhammer showed<sup>30</sup> that this inversion cannot be performed analytically. On the other hand, it is possible to obtain analytical solutions using two-particle Green's-function methods, as developed for the analysis of Auger spectra.<sup>48,49</sup> Unfortunately, these equations are difficult to evaluate and therefore we resort to a numerical method for the calculation of spectral functions, proposed by Gunnarsson and Schönhammer,<sup>47</sup> which is equivalent to the Chebyshev method for the ground state in its performance.

In this method one evaluates the core-hole Green's function in the time domain. One writes

$$G_c(z) = i \int_0^\infty e^{-izt} G_c(t), \quad (25)$$

with

$$G_c(t) = \langle \Psi_c(0) | \Psi_c(t) \rangle, \quad (26)$$

where

$$|\Psi_c(0)\rangle = p_c |\Psi_0\rangle \quad (27)$$

and

$$|\Psi_c(t)\rangle = e^{-iHt/\hbar} p_c |\Psi_0\rangle. \quad (28)$$

$|\Psi_c(t)\rangle$  describes the time evolution of the system after the creation of the core hole. This state satisfies the

time-dependent Schrödinger equation,

$$i\hbar \frac{\delta}{\delta t} |\Psi_c(t)\rangle = H |\Psi_c(t)\rangle, \quad (29)$$

with the initial condition (27).

The state  $|\Psi_c(t)\rangle$  can be expressed in terms of the basis set  $|\underline{c}d^8\rangle$ ,  $|\underline{c}d^9\epsilon\rangle$ , and  $|\underline{c}d^{10}\epsilon\epsilon'\rangle$ , as

$$|\Psi_c(t)\rangle = \sum_j c_j(t) e^{-iH_{jj}t/\hbar} |j\rangle. \quad (30)$$

In order to solve for the coefficients  $c_j(t)$ , one then obtains a system of  $N \times N$  coupled linear differential equations. Using a Runge-Kutta method for this, the calculational effort amounts to a repeated multiplication of the  $\underline{c}(t)$  by the Hamiltonian matrix. As we argued, this requires a relatively small effort. Once the  $c_j(t)$  have been obtained,  $G_c(t)$  can be calculated,

$$G_c(t) = \sum_j c_j^*(0) c_j(t) e^{-H_{jj}t/\hbar}, \quad (31)$$

and the Fourier transform in Eq. (25) can be performed. In practice, we introduce a negative imaginary part in  $z = w - iy$ , which introduces a lifetime broadening in the spectrum in order to cut off the integral (25) at finite  $t$ .

Some results for the core XPS spectrum obtained by this method using  $N_\epsilon = 40$  are shown in Fig. 6. We use parameters representative for Ni compounds ( $U = 5.0$  eV,  $Q = 7.0$  eV,  $W = 3.0$  eV, and  $T = 2.0$  eV) and  $y = 0.6$  eV, introducing a lifetime broadening of 1.2 eV (FWHM) in the spectra. In Fig. 6(a) we show an example of what we called before the strongly ionic regime ( $\Delta = 6$ ), in Fig. 6(b) and 6(c) we show examples of compounds of intermediate covalency ( $\Delta = 3.0$  and 4.0 eV), and in Fig. 6(d) we show an example for a strongly covalent compound ( $\Delta = 1.0$  eV).

In order to get some feeling for the energetics, we have shown in Fig. 7 also the position of the basis states as given by Eqs. (16)–(18). Assuming a hemispherical ligand band, the solid line corresponds with the  $|d^8\rangle$  state [Eq. (16)], the hemisphere with width  $W$  with the  $|d^9\epsilon\rangle$  states, and the hemisphere with width  $2W$  with the  $|d^{10}\epsilon\epsilon'\rangle$  states. Furthermore, we indicate the imaginary part of  $G_{\underline{c}d^8}^{d^8\epsilon}$ . This is the spectral distribution of the  $|\underline{c}d^8\rangle$  state and, as such, is a more direct measure of the electronic structure of the core-ionized state than the XPS spectral function, which is modulated by the overlap with the ground state. For instance, in order to establish the band or bound nature of states, one can better look at  $\text{Im}(G_{\underline{c}d^8}^{d^8\epsilon})$ . Note that  $G_{\underline{c}d^8}^{d^8\epsilon}$  is calculated in the time domain by setting  $|\Psi_c(0)\rangle = |\underline{c}d^8\rangle$ .

We also include in Fig. 6 the results as obtained from the cluster model for the same parameters (solid lines in the spectra). It appears that for all cases the cluster approach is a fair approximation to the full problem. There are, however, some important qualitative differences which are directly related to the band or bound nature of the states involved. As a rule of thumb one can state that if all states which are observed in the spectroscopy are truly bound, the impurity calculation will yield results very similar to the cluster approach. The strongly ionic

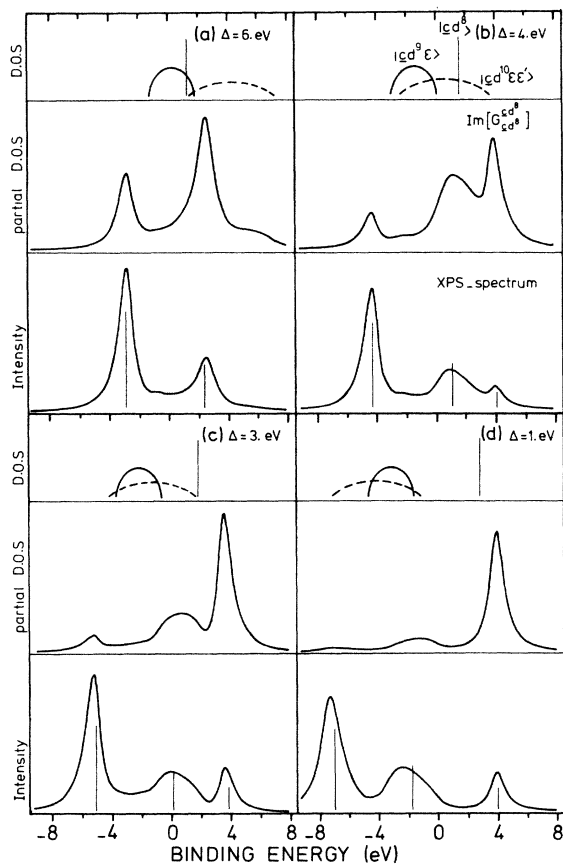


FIG. 6. XPS spectra as derived from the impurity model using  $U=5$  eV,  $Q=7$  eV,  $W=3$  eV,  $T=2$  eV, and  $\Delta$  as indicated. The spectra are broadened with a Lorentzian (FWHM of 1.2 eV) to mimic lifetime broadening. The solid lines drawn in the XPS spectra correspond to the cluster results. Furthermore, we include the energetics of the unhybridized states and the density of states of the  $|cd^8\rangle$  configuration after hybridization [ $\text{Im}(G_{cd^8}^{cd^8})$ ].

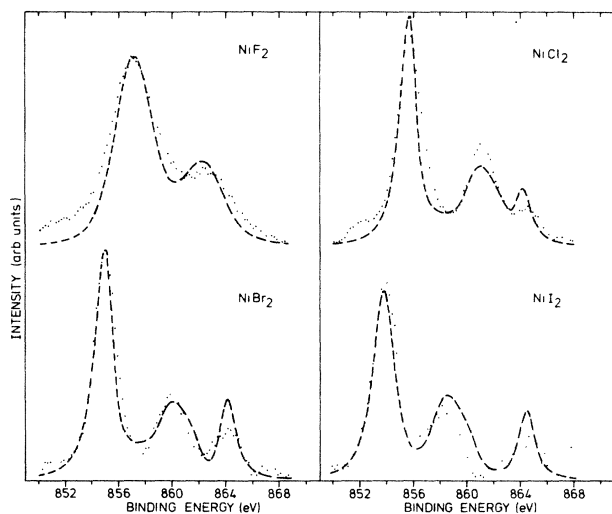


FIG. 7. Fits of the impurity-model results with the experimental  $2p_{3/2}$  spectra of the Ni dihalides. The parameters used can be found in Table II. Besides a Lorentzian lifetime broadening of 1.2 eV, we also included a Gaussian broadening in order to mimic instrumental broadenings of 0.8 eV (FWHM), except for the  $\text{NiF}_2$  spectrum (FWHM of 3.2 eV).

situation as shown in Fig. 6(a) is close to this limit. Lowering  $\Delta$  shifts the  $|d^9\varepsilon\rangle$  and  $|d^{10}\varepsilon\varepsilon'\rangle$  continua to the low-BE side of the spectrum. This has the obvious consequence that the observed features become increasingly more bandlike. From  $\text{Im}(G_{cd^8}^{cd^8})$  one infers that the lowest-BE line corresponds to essentially bandlike states for  $\Delta \lesssim 5$  eV. In these cases one observes differences between the outcomes of the cluster and impurity theory in both the energetics as well as in the intensities.<sup>50</sup>

In the cluster approximation the change in line intensities as a function of a parameter is always rather smooth. In the impurity approximation this is not always true, which can be seen from the sudden uprise from the highest-BE satellite in going from  $\Delta=4$  [Fig. 6(b)] to  $\Delta=3$  [Fig. 6(c)]. For  $\Delta=3$  the highest satellite is truly bound, while for  $\Delta=4$  it is bound with respect to the  $|d^9\varepsilon\rangle$  continuum but not with respect to the  $|d^{10}\varepsilon\varepsilon'\rangle$  continuum. This seems to explain the sudden uprise of the highest-BE satellite in going from  $\text{NiCl}_2$  to  $\text{NiBr}_2$ , which cannot be explained in the cluster approximation.

## V. RESULTS AND DISCUSSION

We used the estimated parameter values appropriate for the Ni dihalide spectra as obtained in Sec. III. We then optimized these values by using the impurity model with a bandwidth ( $W$ ) of 3.0 eV. The best fits to the  $2p_{3/2}$  spectra are shown in Fig. 7. In order to mimic instrumental broadening, we used a Gaussian with 0.8 eV FWHM (except for  $\text{NiF}_2$  with 3.2 eV FWHM) and included a Lorentzian broadening of 1.2 eV in order to mimic lifetime and multiplet effects.

In Table II we present the  $E_{2p_{3/2}}$ ,  $\Delta$ ,  $Q$ ,  $U$ , and  $T$  values as derived in this way. It should be noticed that the only parameter which varies strongly in the series is  $\Delta$ . The monotonic decrease of  $\Delta$  on going from fluoride to iodide is expected from electronegativity arguments. We first notice from Table II that the core-hole energy  $E_{2p_{3/2}}$  [Eq. (9)] is roughly constant across the series, at least compared to the strong shift of the main line to lower BE in going from the fluoride to the iodide. Generally, this kind of shift has been attributed to a lower positive charge on the cation due to increasing covalency with decreasing electronegativity of the anion. From the discussion in Sec. III it is clear that the shift is due to a ligand hole present in the lowest-energy core-hole states, the energy of which shifts according to the anion electronegativity. In the paper of van der Laan *et al.*,<sup>25</sup> it was shown that the same argument holds for the  $\text{Cu(II)}$  halides.

We find that  $Q$  is the largest energy, which is not surprising because in order to have large satellites,  $Q \gg T$ , and to have a large variation in the spectra,  $Q > \Delta$ . We also notice that  $Q$  and  $U$  are approximately constant in the series, which may be surprising at first glance. There are two quantities which can cause  $Q$  to be compound dependent [see Eq. (12)]. First of all, the core-hole–ligand-hole ( $q$ ) interaction can change, and second, the polarization correction ( $2E_p$ ) can change.

We start with the polarization correction. This might be expected to increase as we go from F to I because of

TABLE II. Parameters and ground-state  $d$ -electron counts as determined from the experimental  $2p$  XPS spectra using the impurity theory.

	$\Delta$	$E_{2p_{3/2}}$	$U$	$Q$	$T$	$\langle n_{d^8} \rangle$	$\langle n_{d^9} \rangle$
NiF <sub>2</sub>	6.5	859.8	5	7.0	2.0	0.86	0.14
NiCl <sub>2</sub>	3.6	860.4	5	7.0	2.0	0.72	0.27
NiBr <sub>2</sub>	2.6	860.5	5	7.0	2.0	0.63	0.35
NiI <sub>2</sub>	1.5	860.6	4.5	7.0	2.0	0.51	0.45

the large increase in the polarizability. However, the interatomic spacing increases, which tends to decrease  $E_p$ . In a recent paper this was analyzed for the early-transition-metal compounds.<sup>51</sup> In that paper it was shown that

$$E_p = \frac{1}{2} n \alpha F^2 / \gamma, \quad (32)$$

where  $n$  is the coordination number,  $\alpha$  is the polarizability,  $F = e / 4\pi\epsilon_0 R^2$ , where  $R$  is the interatomic distance, and  $\gamma$  is a factor to correct for the induced-dipole-induced-dipole interaction given by

$$\gamma = 1 + \frac{D\alpha}{4\pi\epsilon_0 R^3}, \quad (33)$$

where  $D$  depends on the crystal structure and is 2.37 for octahedral coordination.

In Table III we have listed the interatomic spacings ( $R$ ),<sup>52</sup> polarizabilities ( $\alpha$ ),<sup>51</sup> and polarization energies  $E_p$  for the four compounds. We see that  $E_p \approx 2.4$  eV and increases by about 0.5 eV in going from F to I. This indicates that  $Q$  should decrease by about 1 eV in going from F to I.

Also given in Table III are the calculated  $2p$ -hole-ligand-hole Coulomb interaction ( $q$ ). To do this we assumed the ligand hole to be localized fully on the first ring of ligands, which is, of course, not entirely so in the real material. We used a point-charge model in a dielectric medium, which, since the charges are well separated in space, is a reasonable way to treat the screening. We then find  $q = 1 / 4\pi\epsilon_\infty R$ . The values of the optical dielectric constant are also listed in Table III. These are derived from the Clausius-Mossotti (CM) equation using the polarizabilities for the anion as listed in Table III and  $\alpha(\text{Ni}) = 0.89$ .<sup>53</sup> For covalent materials the CM relation breaks down and therefore we used, for NiI<sub>2</sub>, the value of  $\epsilon_\infty$  as derived from infrared optical spectroscopy.<sup>54</sup>

We can now make a theoretical estimate for  $Q$ . For this we need values for  $Q_0$  in Eq. (10). We note that, in

contrast to the metals,<sup>55</sup> the Ni  $4s$  electrons cannot provide the screening of the  $d$ - $d$  or  $p$ - $d$  coulomb interactions because of the large  $L$ - $4s$  gap. This is an underlying assumption to Eqs. (4) and (10), and we have to calculate  $Q_0$  from

$$[E_{\text{Cu}}(d^8) - E_{\text{Cu}}(d^9)] - [E_{\text{Ni}}(d^8) - E_{\text{Ni}}(d^9)].$$

We find from Moore's tables<sup>56</sup>  $Q_0 = 18.7$  eV for the free ion. This would correspond to the  $Z + 1$  impurity estimate of  $Q_0$ . Using the configurations  $d^9$  and  $d^{10}$  we obtain 15.5 eV. Since the  $d$  wave functions in the solid are expected to be slightly more diffuse than in the free atom, we prefer the latter estimate. Since the  $2p$ - $3d$  Coulomb interaction is about 1 eV lower than that of a nuclear charge, we arrive at an estimate of  $Q_0 = 14.5$  eV. In Table III the calculated values of  $Q$  are given and we see that  $Q$  is merely constant for the Ni dihalides and has the same order of magnitude as that derived from XPS.

From XPS we find that  $U$  is constant (5 eV) for the compounds, except for the iodide, which gave a somewhat better fit for  $U = 4.5$  eV. In the same way as  $Q$  we can give an estimate for  $U$ . Again,  $U_0$  is determined from Moore's tables<sup>56</sup> from the reaction

$$[E_{\text{Ni}}(d^8) - E_{\text{Ni}}(d^{10})] - 2[E_{\text{Ni}}(d^9) - E_{\text{Ni}}(d^{10})],$$

yielding  $U_0 \approx 12.4$  eV. We note that this number corresponds to the "Hund's rule"  $U_0$ , while the  $U_0$  determined by the core XPS experiments is more akin to the term-averaged  $U_0$ . Using Eq. (32) for  $E_p$  and  $u \approx q$  we then find from Eq. (4) the values of  $U$  listed in Table III. Again we find that  $U$  is approximately constant at 4.6 eV, which nicely fits the experimental value.

From Table II we notice that the transfer integral is approximately constant at 2 eV across the series. This also is expected, since although the radial extent of the I  $5p$  orbital is considerable larger than that of the F  $2p$  orbital, the lattice parameters are also much larger. In much earlier work by one of us, it was shown that the  $3d$ - $L$  overlap integral is nearly constant for the Fe halides precisely be-

TABLE III. Theoretical estimates for  $U$  and  $Q$  using polarization and ligand-hole-metal-hole Coulomb interaction corrections.

	$\alpha$ ( $\text{\AA}^3$ )	$R$ ( $\text{\AA}$ )	$\epsilon_\infty$	$E_p$ (eV)	$q$ (eV)	$Q$ (eV)	$U$ (eV)
NiF <sub>2</sub>	1.2	2.0	3.74	2.39	1.92	7.8	4.7
NiCl <sub>2</sub>	3.0	2.46	3.56	2.39	1.63	8.1	4.4
NiBr <sub>2</sub>	4.5	2.58	4.97	2.71	1.12	8.0	4.7
NiI <sub>2</sub>	7.0	2.78	6.00	2.86	0.87	7.9	4.6

cause of the above canceling changes.<sup>57</sup>

As we showed in a parallel paper, the  $2p$  absorption spectra of the Ni dihalides can be analyzed within the same model.<sup>41</sup> We there showed that the absorption spectra are very sensitive to the values of  $\Delta - Q + U$  and  $T$ . Comparison of the values for these quantities as derived from both spectroscopies shows that the values of  $\Delta - Q + U$  are in good mutual agreement, but from x-ray-absorption spectroscopy (XAS) a considerably smaller value is found for  $T$  (1.5 eV) than from XPS (2 eV). The large value coming from the analysis of XPS is mainly suggested by the relative intensities; for  $T=1.5$  eV a slightly different set of parameters can be defined for all cases, yielding a good fit to the final-state line positions, but then overly large satellites are found. Very much the same problem with  $T$  is found in the analysis of the spectra of Ce intermetallics, where Hillebrecht *et al.*<sup>58</sup> find that  $1/N$  theory<sup>30</sup> (which is very close to our theory) predicts considerably larger values for the hybridization parameters for core XPS (Ref. 34) than for valence-band spectroscopy. Although we do not think that we are able to give the final solution to this problem, here we will point out an effect which at least works into the right direction.

In the model we assumed Coulomb interactions of the form

$$\Delta T = \left\langle \underline{c} \left| d \right| \frac{1}{r_{12}} \left| L\underline{c} \right\rangle$$

to be zero. This type of Coulomb interaction will cause the transfer integral to be different in the presence of the core hole. We can estimate the size of this as follows. We consider the core hole as an extra nuclear charge, so we can write

$$\Delta T \simeq \left\langle \Psi_d(r) \left| \frac{e}{r} \right| \Psi_L(r-R) \right\rangle,$$

where  $R$  is the interatomic spacing. This will have contributions mainly in the overlap region of  $\Psi_d(r)$  and  $\Psi_L(r-R)$ , so, by approximation,

$$\Delta T \simeq \frac{2e}{R} \langle \Psi_d(r) | \Psi_L(r-R) \rangle,$$

and since  $R \simeq 2$  Å and the overlap integral is about 0.05, we get  $\Delta T \simeq 0.7$  eV. This shows that  $T$  in the presence of the core hole can be considerably larger than that which should be used to describe the valence-band spectroscopies. Also, using the same arguments the matrix elements  $\langle \underline{c}d^8 | H | \underline{c}d^9\underline{L} \rangle$  will be larger than  $\langle \underline{c}d^9\underline{L} | H | \underline{c}d^{10}\underline{L} \rangle$  in which the core hole is screened by the extra  $d$  electron and, therefore, this  $T$  should be close to the one for the valence band,  $\langle d^8 | H | d^9\underline{L} \rangle$ . This would suggest that  $\Delta T \simeq 0.5$  eV; in other words, that in the initial state we should use  $T=1.5$  eV and, in the core-ionized state,  $T=2$  eV. In order to quantify this, we compare in Fig. 8 the NiBr<sub>2</sub> spectrum as derived from  $T_{\text{init}}=T_{\text{ion}}=2$  eV [Fig. 8(c)] with the same spectrum with  $T_{\text{init}}=1.5$  eV and  $T_{\text{ion}}=2$  eV [Fig. 8(b)] and the spectrum derived from  $T_{\text{init}}=T_{\text{ion}}=1.5$  eV [Fig. 8(a)]. From this one can see that although the  $\Delta T$  effect works into the right direction, it is not sufficient to bring the satellite in-

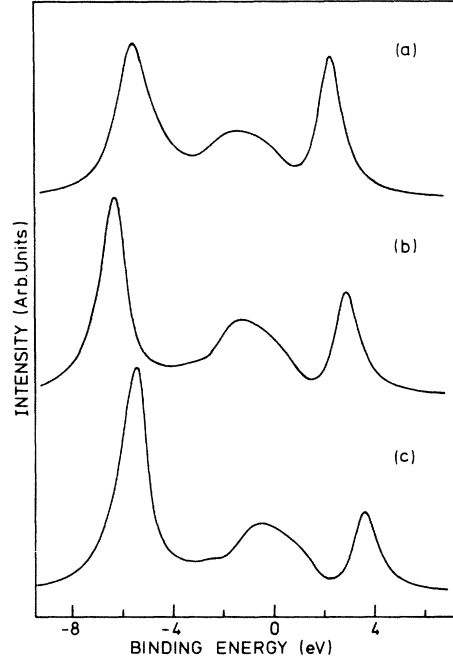


FIG. 8. The influence of a different  $T$  in ground and core-ionized state. We used the same parameters as for NiBr<sub>2</sub>, and in (a) we used  $T(\text{neutral})=T(\text{ion})=1.5$  eV; in (b),  $T(\text{neutral})=1.5$  eV and  $T(\text{ion})=2$  eV; and in (c),  $T(\text{neutral})=T(\text{ion})=2$  eV.

tensities down to the measured ones. Taking the uncertainty in the origin of the peak intensities into account, it will be clear that one should not take the parameter values as listed in Table II too literally. We expect that the error in all parameters is typically on the order of 0.5 eV.

Having gained some faith in the parameter values as determined by core XPS, it is interesting to see how these relate to the electronic properties of these systems, namely the ground-state electronic structure and the conductivity gaps.

With respect to the ground state the important quantity is the charge (and spin) distribution. The ground-state values for the  $d^8$  and  $d^9$  counts found from our analysis are included in Table II. As we expected, NiF<sub>2</sub> is strongly ionic with a  $d$ -electron count very close to eight, NiI<sub>2</sub> is almost purely covalent, and NiBr<sub>2</sub> and NiCl<sub>2</sub> are in between.

To our knowledge no attempts have been undertaken to determine the ground-state  $d$ -electron counts by other experiments. It makes sense, however, to compare these values with the ones found from local-density band-structure calculations because these calculations are expected to be quite good for the ground state. Although the  $d$ -electron counts in band-structure calculations depend strongly on the muffin-tin radius and are therefore ill defined, it is convincing that the  $d$ -electron counts found using a reasonable muffin-tin radius (1.3 Å) in an augmented-spherical-wave calculation<sup>39</sup> are very close to those we have determined from core XPS.

Things work less well when we consider the conduction-band gap. We showed before<sup>6</sup> that the conduction-band gap in Ni compounds is expected to be either of Mott-Hubbard ( $E_{\text{gap}} \propto U$ ) or charge-transfer

( $E_{\text{gap}} \simeq \Delta - \frac{1}{2}W$ ) nature. If we then compare the band-gap magnitudes as measured by photoconductivity [NiCl<sub>2</sub>, NiBr<sub>2</sub>, and NiI<sub>2</sub> with, respectively, 4.0, 3.2, and 1.7 eV (Ref. 59)] with the core XPS parameters, there is obviously a problem. Recalling the analogy with NiO,<sup>3</sup> the trend in the band-gap magnitude suggests that NiCl<sub>2</sub>, NiBr<sub>2</sub>, and NiI<sub>2</sub> are predominantly charge-transfer semiconductors. Using then the core XPS values for  $\Delta$ , we would consequently find band gaps 2.0 eV smaller than the experimental band gaps.

There is also experimental evidence that the "ground-state"  $U(d^8 \rightarrow d^{10})$  is different from the "Mott-Hubbard"  $U(d^7 \rightarrow d^9)$ , as required for the determination of the gaps and the valence-band (inverse-) photoemission spectra. Being all insulators, we would expect that the  $U(d^7 \rightarrow d^9)$  in the halides to be roughly the same as the  $U(d^7 \rightarrow d^9)$  of NiO, i.e., typically 8.0 eV, which is considerably larger than the core XPS  $U$ 's ( $\approx 4.5$ – $5$  eV) (also see Ref. 60).

The preceding discussion indicates that the parameters in the model Hamiltonian depend on the specific experiment to be analyzed. This is, of course, not surprising since the Hamiltonian [Eq. (14)] is highly "effective" and, to a certain extent, these mismatches can be understood.

In the first place, one can try to improve the modeling of the quantities included in Eq. (14); for instance, it is quite crude to model the hybridization with the ligand states with a hemisphere and it can very well be that the appropriate effective ligand bandwidth (of TM  $d$  symmetry) for the Ni dihalides is considerably smaller than the choice we made. We also note that the exchange is treated in quite a rough way in the calculation of the band gap and the core XPS spectrum.

More demanding are the effects of the interactions, which are not explicitly included in the model Hamiltonian. We first consider local (atomic) effects. For instance, the bare  $U$  related to the band-gap magnitude has to be calculated from

$$\begin{aligned} U_0(d^7 \rightarrow d^9) &= [E_{\text{Ni}}(d^7) - E_{\text{Ni}}(d^8)] + [E_{\text{Ni}}(d^9) - E_{\text{Ni}}(d^8)] \\ &= 17.0 \text{ eV} \end{aligned}$$

(Ref. 56), considerably larger than the  $U_0(d^8 \rightarrow d^{10})$  needed for the ground-state and core XPS.

Furthermore, we have the nonlocal interactions such as the polarization energy ( $E_p$ ) and the  $d$ -electron–ligand-hole interaction ( $u$ ), which we discussed before. It can be seen immediately that  $u$  can give rise to different effective  $\Delta$ 's; as we discussed, in the ground-state and the core XPS the ligand hole is more or less localized in the vicinity of the  $d$  electron, which will tend to reduce  $\Delta$  as compared to the conduction-band gap  $\Delta$  where we imposed the  $d$  electron and ligand hole to be uncorrelated. We believe that this, at least in part, explains the large  $\Delta$ 's needed in gap calculations.

As we discussed, the ligand-hole– $d$ -electron Coulomb interaction will also reduce  $U(d^8 \rightarrow d^{10})$ . This interaction will, on the other hand, not affect  $U(d^7 \rightarrow d^9)$ , which will tend to make the difference between these  $U$ 's even more pronounced. We note that the near constancy of  $U(d^8 \rightarrow d^{10})$  in this picture is due to the partial cancella-

tion of the increase of  $E_p$  by the decrease of  $u$  in going from the fluoride to the iodide. For  $U(d^7 \rightarrow d^9)$  this cancellation does not occur and a stronger variation of this  $U$  is expected.

## VI. CONCLUSIONS

We have presented  $2p$  XPS spectra of the Ni dihalides and we have compared these with the outcomes of a recently proposed many-body theory for insulating transition-metal compounds. We showed that all experimental trends were reproduced by the theory. Furthermore, we showed that the simple cluster approximation is a fairly good approximation to the full theory and certainly useful for a rough characterization of the parameters which determine the valence-electronic structure.

By means of a detailed comparison between theory and experiment, we obtained values for these parameters. We found that the  $d$ - $d$  ( $U$ ) and  $p$ - $d$  ( $Q$ ) Coulomb interactions are roughly constant over the series. We confirmed that these energies are the largest energies present in these systems. We showed that the values of  $U$  and  $Q$  as derived from XPS were of the same order as theoretical estimates based on bare Coulomb interactions corrected for polarization and metal- ( $p, d$ ) hole–ligand-hole Coulomb interactions. We also found that the  $p$ - $d$  transfer integral is roughly constant for the different halides.

We found that the charge-transfer energy  $\Delta$  is the quantity which is strongly altered in going through the neptalutix series. This is in qualitative agreement with the behavior of the (optical) gap in these materials.

Comparing quantitatively the parameters found from core XPS with results for the band gap and the x-ray-absorption spectrum, we find systematic discrepancies. We argue that this is due to the effective nature of the used Hamiltonian in which the renormalization of the parameters depends more or less on the experiment. We argue that the parameters  $U$  and  $\Delta$  are similar for the ground-state and core XPS calculations, whereas both  $U$  and  $\Delta$  are larger in the conductivity-gap calculation. First-principles calculations are needed to shed more light on this matter.

## ACKNOWLEDGMENTS

The authors thank Professor C. Haas and Dr. D. van der Marel for helpful discussions. This investigation was supported by the Netherlands Foundation for Chemical Research [Stichting Scheikundig Onderzoek Nederland (SON)] with financial aid from the Netherlands Organization for the Advancement of Pure Research [Nederlandse Organisatie voor Zuiver-Wetenschappelijk Onderzoek (ZWO)].

## APPENDIX

In this appendix we present and work out a good approximation to the ground-state wave function for large  $U$ 's.

As Gunnarsson and Schönhammer discussed in their papers,<sup>30,47</sup> their "folding" technique breaks down in the presence of double occupied states, because the folding of

$|d^{10}\epsilon\epsilon'\rangle$  produces nondiagonal elements between  $|d^9\epsilon\rangle$  states.

There is a simple approximation to the coupling between  $|d^9\epsilon\rangle$  and  $|d^{10}\epsilon\epsilon'\rangle$  states which removes this problem. Instead of (20b) we write

$$\langle d^9\epsilon | H_{\text{imp}} | d^{10}\epsilon'\epsilon'' \rangle = \delta(\epsilon - \epsilon') \sqrt{2} V(\epsilon''), \quad (\text{A1})$$

and we consider  $\epsilon'$  and  $\epsilon''$  to be distinguishable. We express the ground state as

$$|\Psi_c\rangle = A \left[ |d^9\rangle + \int_{-W/2}^{W/2} d\epsilon a(\epsilon) |d^9\epsilon\rangle + \int_{-W/2}^{W/2} d\epsilon \int_{-W/2}^{W/2} d\epsilon' b(\epsilon, \epsilon') |d^{10}\epsilon\epsilon'\rangle \right], \quad (\text{A2})$$

with

$$A = \left[ 1 + \int_{-W/2}^{W/2} d\epsilon |a(\epsilon)|^2 + \int_{-W/2}^{W/2} \int_{-W/2}^{W/2} |b(\epsilon, \epsilon')|^2 d\epsilon d\epsilon' \right]^{-1/2}. \quad (\text{A3})$$

Using the variational principle now yields straightforward results. We find, for the ground-state energy (relative to

$$\langle d^8 | H_{\text{imp}} | d^8 \rangle = 0),$$

$$\delta = \sqrt{2} \int_{-W/2}^{W/2} d\epsilon V^*(\epsilon) a(\epsilon), \quad (\text{A4})$$

$$[\delta - \Delta - \epsilon - \Gamma(\delta - 2\Delta - U - \epsilon)] a(\epsilon) = \sqrt{2} V(\epsilon), \quad (\text{A5})$$

with

$$\Gamma(\epsilon) = 2 \int_{-W/2}^{W/2} \frac{|V(\epsilon')|^2 d\epsilon'}{\epsilon - \epsilon'}. \quad (\text{A6})$$

The ground-state energy is thus given by the transcendental equation

$$\delta = 2 \int_{-W/2}^{W/2} \frac{d\epsilon |V(\epsilon)|^2}{\delta - \Delta - \epsilon - \Gamma(\epsilon - 2\Delta - U - \epsilon)}. \quad (\text{A7})$$

Furthermore, because

$$b(\epsilon, \epsilon') = \frac{\sqrt{2} V(\epsilon) a(\epsilon)}{\delta - 2\Delta - U - \epsilon - \epsilon'}, \quad (\text{A8})$$

the ground-state occupation numbers can be calculated. Calculations show that the ground-state wave function and energy are very close to the exact numerical result obtained in Sec. III, at least for  $\Delta + U \gtrsim W$ .

- <sup>1</sup>K. Terakura, A. R. Williams, T. Oguchi, and J. Kuebler, *Phys. Rev. Lett.* **52**, 1830 (1984); K. Terakura, T. Oguchi, A. R. Williams, and J. Kuebler, *Phys. Rev. B* **30**, 4734 (1984).
- <sup>2</sup>A. Fujimori, F. Minami, and S. Sugano, *Phys. Rev. B* **29**, 5225 (1984); A. Fujimori and F. Minami, *ibid.* **30**, 957 (1984).
- <sup>3</sup>G. A. Sawatzky and J. W. Allen, *Phys. Rev. Lett.* **53**, 2339 (1984); S. Hüfner, J. Osterwalder, T. Riesterer, and F. Hüfner, *Solid State Commun.* **52**, 793 (1984); J. M. McKay and V. E. Henrich, *Phys. Rev. Lett.* **53**, 2343 (1984).
- <sup>4</sup>N. F. Mott, *Proc. Phys. Soc. (London), Sect. A* **62**, 416 (1949); *Can. J. Phys.* **34**, 1356 (1956); *Philos. Mag.* **6**, 287 (1961).
- <sup>5</sup>J. Hubbard, *Proc. R. Soc. London, Ser. A* **277**, 237 (1964); **281**, 401 (1964).
- <sup>6</sup>J. Zaanen, G. A. Sawatzky, and J. W. Allen, *Phys. Rev. Lett.* **55**, 418 (1985); *J. Magn. Magn. Mater.* **54-57**, 607 (1986).
- <sup>7</sup>P. W. Anderson, *Phys. Rev.* **115**, 2 (1959); *Magnetism*, edited by G. Radon and H. Suhl (Academic, New York, 1963) Vol. 1, p. 25; in *Solid State Physics*, edited by F. Seitz and D. Turnbull (Academic, New York, 1963), Vol. 14, p. 95.
- <sup>8</sup>A. Rosenzweig, G. K. Wertheim, and H. J. Guggenheim, *Phys. Rev. Lett.* **27**, 479 (1971).
- <sup>9</sup>D. C. Frost, C. A. McDowell, and I. S. Woolsey, *Chem. Phys. Lett.* **17**, 320 (1972).
- <sup>10</sup>L. J. Matienzo, L. I. Yin, S. O. Grim, and W. E. Swartz, *Inorg. Chem.* **12**, 2762 (1973).
- <sup>11</sup>S. Hüfner and G. K. Wertheim, *Phys. Rev. B* **8**, 4857 (1973).
- <sup>12</sup>B. Wallbank, C. E. Johnson, and I. G. Main, *J. Phys.* **6**, L340 (1973).
- <sup>13</sup>T. A. Carlson, J. C. Carver, L. J. Saethre, F. Garcia Santibanez, and G. A. Vernon, *J. Electron Spectrosc. Relat. Phenom.* **5**, 259 (1974).
- <sup>14</sup>B. Wallbank, I. G. Main, and C. E. Johnson, *J. Electron Spectrosc. Relat. Phenom.* **5**, 259 (1974).
- <sup>15</sup>K. S. Kim and R. E. Davis, *J. Electron Spectrosc. Relat. Phenom.* **3**, 217 (1974).
- <sup>16</sup>T. A. Carlson, J. C. Carver, and G. A. Vernon, *J. Chem. Phys.* **62**, 932 (1975).
- <sup>17</sup>M. A. Brisk and A. D. Baker, *J. Electron Spectrosc. Relat. Phenom.* **6**, 81 (1975).
- <sup>18</sup>K. S. Kim, *Phys. Rev. B* **11**, 2177 (1975).
- <sup>19</sup>S. Larsson, *Chem. Phys. Lett.* **32**, 401 (1975).
- <sup>20</sup>S. Larsson, *Chem. Phys. Lett.* **40**, 362 (1976).
- <sup>21</sup>S. Asada and S. Sugano, *J. Phys. Soc. Jpn.* **41**, 1291 (1976).
- <sup>22</sup>G. A. Vernon, G. Stucky, and T. A. Carlson, *Inorg. Chem.* **15**, 278 (1976).
- <sup>23</sup>M. Scrocco, *J. Electron Spectrosc. Relat. Phenom.* **19**, 311 (1980).
- <sup>24</sup>G. van der Laan, C. Westra, C. Haas, and G. A. Sawatzky, *Phys. Rev. B* **23**, 4369 (1981).
- <sup>25</sup>S. Asada and S. Sugano, *J. Phys. Soc. Jpn.* **41**, 1291 (1976).
- <sup>26</sup>B. W. Veal and A. P. Paulakis, *Phys. Rev. Lett.* **51**, 1995 (1983).
- <sup>27</sup>S. Hüfner, *Solid State Commun.* **47**, 943 (1983).
- <sup>28</sup>S. Hüfner, *Solid State Commun.* **49**, 1177 (1984).
- <sup>29</sup>B. W. Veal and A. P. Paulakis, *Phys. Rev. B* **31**, 5399 (1985).
- <sup>30</sup>O. Gunnarsson and K. Schönhammer, *Phys. Rev. Lett.* **50**, 604 (1983); *Phys. Rev. B* **28**, 4315 (1983).
- <sup>31</sup>A. Fujimori, *Phys. Rev. B* **27**, 3992 (1983); **28**, 2281 (1983); **28**, 4489 (1983).
- <sup>32</sup>E. Wuilloud, B. Delley, W. D. Schneider, and Y. Baer, *Phys. Rev. Lett.* **53**, 202 (1984).
- <sup>33</sup>A. Kotani, H. Mizuta, and T. Jo, *Solid State Commun.* **53**, 805 (1985).
- <sup>34</sup>J. C. Fuggle, F. U. Hillebrecht, Z. Zołnier, R. Lasser, Ch. Freiburg, O. Gunnarsson, and K. Schönhammer, *Phys. Rev. B* **27**, 7330 (1983).
- <sup>35</sup>I. Pollini, J. Thomas, G. Jezequel, J. C. Lemonnier, and R. Mamy, *Phys. Rev. B* **27**, 1303 (1983); I. Pollini, J. Rhomas, and A. Lenselink, *ibid.* **30**, 2140 (1984).
- <sup>36</sup>E. Antonides, Ph.D. thesis, Laboratory of Physical Chemistry,

- Groningen (1977).
- <sup>37</sup>J. Zaanen and G. A. Sawatzky, following paper, *Phys. Rev. B* **33-I**, 8074 (1986).
- <sup>38</sup>See Fig. 2 in Ref. 57.
- <sup>39</sup>R. Coehoorn, Ph.D. thesis, Laboratory of Physical Chemistry, Groningen (1985).
- <sup>40</sup>A. Bringer and H. Lustfeld, *Z. Phys. B* **28**, 213 (1977).
- <sup>41</sup>G. van der Laan, J. Zaanen, and G. A. Sawatzky, *Solid State Commun.* **56**, 673 (1985); *Phys. Rev. B* **33**, 4253 (1986).
- <sup>42</sup>R. P. Gupta and S. K. Sen, *Phys. Rev. B* **12**, 15 (1975).
- <sup>43</sup>R. Rekha, S. Pal, and R. P. Gupta, *Phys. Rev. B* **26**, 35 (1982).
- <sup>44</sup>S. Asada, C. Satoka, and S. Sugano, *J. Phys. Soc. Jpn.* **38**, 855 (1975).
- <sup>45</sup>S. Asada and S. Sugano, *J. Phys. Soc. Jpn.* **41**, 1291 (1976).
- <sup>46</sup>S. P. Kowalczyk, L. Ley, F. R. McFeely, and D. A. Shirley, *Phys. Rev. B* **11**, 1721 (1975).
- <sup>47</sup>O. Gunnarsson and K. Schönhammer, *Phys. Rev. B* **31**, 4815 (1985).
- <sup>48</sup>M. Vos, D. van der Marel, and G. A. Sawatzky, *Phys. Rev. B* **29**, 3073 (1984).
- <sup>49</sup>V. Drchal and J. Kudrnovsky, *Phys. Status Solidi B* **108**, 683 (1981).
- <sup>50</sup>See also A. Fujimori, *Phys. Rev. Lett.* **53**, 2518 (1984); E. Wuilloud, B. Delley, W. D. Schneider, and Y. Baer, *ibid.* **53**, 2519 (1984).
- <sup>51</sup>D. K. G. de Boer, C. Haas, and G. A. Sawatzky, *Phys. Rev. B* **29**, 4401 (1984).
- <sup>52</sup>*Gmelin's Handbuch der Anorganische Chemie* (Verlag Chemie GmbH, Weinheim, West Germany, 1966), Vol. 57B2.
- <sup>53</sup>I. Pollini, G. Benedek, and J. Thomas, *Phys. Rev. B* **29**, 3617 (1984).
- <sup>54</sup>S. R. Kuindersma, *Phys. Status Solidi B* **107**, K163 (1981); Ph.D. thesis, University of Groningen (1984).
- <sup>55</sup>C. Herring, in *Magnetism, Vol. IV*, edited by T. Rado and H. Suhl (Academic, New York, 1964).
- <sup>56</sup>C. E. Moore, *Atomic Energy Levels*, NBS circular No. 467 (U.S. GPO, Washington, D.C., 1958), Vols. 1–3.
- <sup>57</sup>G. A. Sawatzky and F. van der Woude, *J. Phys. (Paris) Colloq.* **35**, C6-47 (1974).
- <sup>58</sup>F. U. Hillebrecht, J. C. Fuggle, G. A. Sawatzky, M. Campagna, O. Gunnarsson, and K. Schönhammer, *Phys. Rev. B* **30**, 1777 (1984).
- <sup>59</sup>C. R. Ronda and G. J. Arends, unpublished results.
- <sup>60</sup>S. Hufner, *Solid State Commun.* **53**, 707 (1985).